NMR Applications for Identifying β-TrCP Protein-Ligand Interactions

J. Pons[§,1], V. Tanchou[2], J.-P. Girault[1], G. Bertho[1] and N. Evrard-Todeschi*[,1]

[1]*Université Paris Descartes, Laboratoire de Chimie et Biochimie Pharmacologiques et Toxicologiques (UMR 8601 CNRS), 45 rue des Saints-Pères, 75270 Paris Cedex 06, France*

[2]*CEA ValRhô – Direction des Sciences du Vivant – Institut de Biologie Environnementale et Biotechnologie – Service de Biochimie et Toxicologie Nucléaire, BP1717, 30207 Bagnols sur Cèze, France*

Abstract: In the absence of crystallographic data, NMR has emerged as the best way to define protein-ligand interactions. Using NMR experiments based on magnetization transfer, one can sort bound from unbound molecules, estimate the dissociation constant, identify contacts implied in the binding, characterize the structure of the bound ligand and conduct ligand competition assays.

Keywords: STD-NMR, WaterLOGSY, epitope mapping, docking, phosphorylated peptide, β-TrCP complex, binding fragment.

1. INTRODUCTION

Nuclear magnetic resonance (NMR) spectroscopy has become a powerful tool for identifying compounds in interaction with macromolecules. This technique is used to understand the binding mode and identify drug candidates in the drug discovery process. NMR has assumed an important role in the detection of weak and transient interactions, in the investigation of atomic contacts, and in the characterization of protein interactions with small molecules. In recent years, NMR screening has been consistently used in target-directed drug discovery programs [1]. Numerous applications have been developed for the screening of small molecules against the target of interest. These include differential line broadening, NOE pumping [2], reverse NOE pumping [3], water-ligand observed *via* gradient spectroscopy (WaterLOGSY) [4] and saturation transfer difference (STD) [5]. These experiments are based on different properties between the bound and the free compounds such as diffusion rate and relaxation rate, chemical shifts, and the sign and intensity of NOEs. In addition, transferred nuclear Overhauser effects (TRNOEs) permit to obtain structural information on the bound conformation [6].

NMR can be used to screen compound libraries to detect ligands by using these methods; various data can be exploited. Indeed, the interaction is easily detected when comparing for example the line broadening of the free compound (weaker line broadening) and that of the compound in presence of the receptor (larger line broadening). The dissociation constant, K_d, can be determined using a simple protocol [7, 8], based on titration of the ligand. One can precisely determine the atoms implied in the interaction and then characterize an epitope mapping of the interaction by using saturation transfer difference NMR (STD-NMR) [5, 8, 9]. If the structure of the macromolecule is available, a docking process may be conducted to determine the interaction site, consistent with the NMR data.

We set out to address the important question of the competition between substrates for binding to a macromolecule. One can perform a competition STD-NMR method, which extends the STD-NMR with competitive binding and allows the detection of the higher affinity ligand for the same binding site [10]. This method can also be used to derive a lower limit for the dissociation constant of the ligand [10]. This STD-NMR method can be extended to rank order analogues and derive structure-activity relationships.

The ability to characterize protein-ligand interactions using STD, WaterLOGSY NMR experiments is demonstrated in an example with β-Transducin repeat Containing Protein (β-TrCP) that plays a key role on protein degradation by the proteasome. The ubiquitin-proteasome pathway regulates gene expression through protein degradation. The role of β-TrCP in the Skp1-Cdc53-F-box protein (SCF) ubiquitin ligase complex is to select and recruit the proper substrate for polyubiquitination by the SCF complex. Proteasome-mediated protein degradation requires the covalent attachment of polyubiquitin to the substrate proteins [11-13]. The binding activity of β-TrCP is due to the seven WD-40 repeats at the C terminus-recognition domain (Fig. (**1**)). The protein-protein interactions involved can be simulated by a short peptide. The three-dimensional structure of the human β-TrCP-Skp1 complex bound to a β-catenin peptide has been determined by X-ray crystallography [14]. Preliminary results on mapping the binding epitope of β-TrCP ligands (Vpu, IκB-α, β-catenin and ATF4) had been previously published [15-18]. These ligands share a

*Address correspondence to this author at the Université Paris Descartes, Laboratoire de Chimie et Biochimie Pharmacologiques et Toxicologiques (UMR 8601 CNRS), 45 rue des Saints-Pères, 75006 Paris, France;
Tel: 33-1-42-86-21-82; Fax: 33-1-42-86-83-87;
E-mail: nathalie.evrard-todeschi@parisdescartes.fr

[§]Moved to: Université de Lyon, Université Claude BERNARD - Lyon 1, Sciences Analytiques, CNRS UMR 5180, Domaine scientifique de la Doua, ESCPE-Lyon, 69622 Villeurbanne, France.

1389-5575/11 $58.00+.00

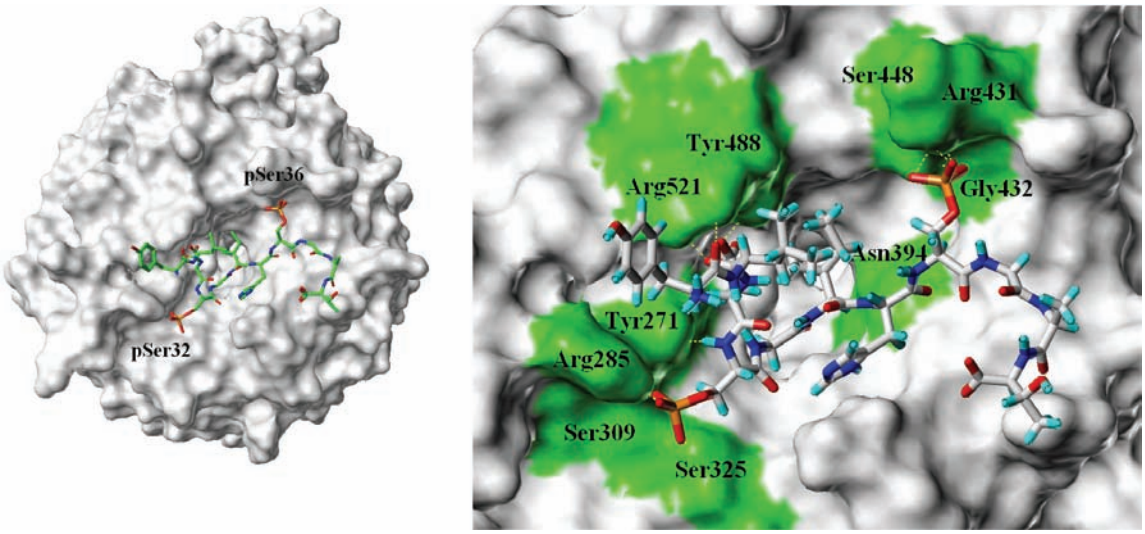

Fig. (1). A) Surface representation of the top face of the *β*-TrCP WD40 domain with the bound *β*-catenin peptide. **B**) Close-up view of the interface between the *β*-TrCP WD40 domain and the doubly phosphorylated peptide ligand [14, 18]. Essential amino acids involved in the interaction are shown in the green surface.

Table 1. Bound Structures of the β-TrCP Peptide Ligands. Sequence of Five Peptide Ligands of the *β*-TrCP Protein. These Structures have been Used for Binding Mode Prediction

Name	Sequence number	Sequence	Source	Ref
11P-*β*-catenin	30-40	YL**DSGIHS**GAT	X-ray	[14, 15]
22P-Vpu	41-62	LIDRLIERAE**DSGNES**EGEISA	NMR[a]	[15]
32P-*β*-catenin	19-44	DRKAAVSHWQQQSYL**DSGIHS**GATTTAPSLSG	NMR[a]	[16]
24P-IκBα	21-44	KKERLLDDRH**DSGLDS**MKDEEYEQ	NMR[a]	[17]
23P-ATF4	208-230	IKEEDTPSDN**DSGICMS**PESYLG	NMR[a]	[18]

[a]minimized average structure.

common motif, D**pS**G(*X*)$_n$**pS** and phosphorylation of their serine residues are required for interaction with the *β*-TrCP protein (Table **1**). The conformations of the peptides in the *β*-TrCP complex are almost identical but significant differences were observed for the orientation and conformation of the phosphorylated serine residues in the binding pocket. For instance, the NMR data unambiguously show that the conformation of the ligand bound structure presents a bend corresponding to the D**pS**G(*X*)$_n$**pS** motif.

In this paper, we report results of interaction between *β*-TrCP and the different ligands Viral protein U (Vpu), Activating Transcription Factor 4 (ATF4), Inhibitor of nuclear factor kappa B alpha (IκB-α) and *β*-catenin. The complexes were studied by Biacore, by Fluorescence and by NMR techniques (chemical shift, STD and WaterLOGSY methods), and finally the NMR appears to be a powerful tool to characterize weak interactions, such as the *β*-TrCP ligand system presents. A comparison between the NMR results and the crystallographic results complements our understanding of the respective *β*-TrCP binding modes.

Moreover, the docking of ligands into an assembly of NMR bound conformers presented in Table 1 (23P-ATF4, 22P-Vpu, 24P-IκBα, and 32P-*β*-catenin) is essential to predict ligand binding modes and to consider *β*-TrCP protein structure variations in ligand binding. X-ray structures of the proteins in interaction with the *β*-TrCP protein cannot be obtained: although only NMR bound structures determined in solution are available for the target, the proteins cannot be crystallized.

2. METHODOLOGY

2.1. Purification of the WD Repeat Region from Human Protein β-TrCP fused to the Maltose Binding Protein (MBP)

Coding sequence corresponding to the 253-547 residues of full-length protein *β*-TrCP was inserted into the pMAL-C2X expression vector (OZYME). The construction resulted in a fusion protein of approximately 75 kDa corresponding to the 361 residues of the MBP [19], a 33-mer linker and the seven WD repeats (residues 253-547) of *β*-TrCP hereafter named MBP-*β*-TrCP. Protein concentration was determined using the standard Bradford method following the OD at 595 nm. At last, the purified recombinant protein was concentrated using Amicon Ultra-15 centrifugal filter units (Millipore) with a 10 kDa molecular weight cut-off and

dialyzed in NMR buffer in order to remove maltose. Following this protocol, the final yield of purified MBP-*β*-TrCP was of 3.5 mg/ml. This amount of purified recombinant protein was used to prepare the NMR samples.

2.2. NMR Spectroscopy

All NMR spectra were carried out on Bruker AVANCE 500 spectrometer equipped with a 5 mm TXI triple resonance probe including shielded *z*-gradients. In all experiments, the temperature was maintained at 280 ± 0.1 K. Standard 5 mm NMR tubes or Shigemi tubes for low volumes matched for ^2H_2O were used.

The NMR samples were in ^2H_2O or $H_2O/^2H_2O$ 9:1 (v/v) with 50 mM phosphate buffer solution, pH 7.2. ^2H_2O was added to the solutions (10% final concentration) for the lock signal. Sodium 3–trimethylsilyl (2,2,3,3–$^2H_4$) propionate was used as internal reference for the proton shifts. Two-dimensional NMR spectra were recorded in the phase-sensitive mode using the time proportional phase incrementation (States-TPPI) method [20] for quadrature detection in the t_1 dimension. All experiments were carried out with water suppression using the excitation sculpting pulse sequence [21] or using the Water Suppression by Gradient-Tailored Excitation (WATERGATE) [22] to eliminate solvent signal in $H_2O/^2H_2O$ 9:1 solution. The following conventional two-dimensional experiments IP-COSY [23], total correlation spectroscopy (TOCSY) [24], nuclear Overhauser effect spectroscopy (NOESY) [25], and rotating-frame Overhauser enhancement spectroscopy (ROESY) [26] spectra were recorded at 280 K. For the two-dimensional $^1H,^1H$ IP-COSY spectra, a mixing time of 50 ms and constant time of 15 ms were applied. A 54°-shifted sine-squared bell window function (SSB=3.333) was used in the *F2* dimension for IP-COSY and a squared cosine in the *F1* dimension. Water suppression was achieved by excitation sculpting. A trim pulse (2.5 ms) was used to remove *F2* anti-phase components in IP-COSY [23]. TOCSY spectra were recorded using a MLEV-17 spin–lock sequence [27] with a mixing time (τ_m) of 35 and 70 ms, respectively. For two-dimensional phase sensitive NOESY experiments an optimal mixing time of 300 ms was observed in the 50–500 ms range. For ROESY experiments, a spin–lock of 50–400 ms was used. The spectra were recorded with 512(t_1) x 4096(t_2) data points and with a proton spectral width of 5482.5 Hz in water. Spectra were analyzed with FELIX (Accelrys) software and chemical shift assignments were done manually, using data from TOCSY and NOESY experiments.

^1H resonance assignments and spectral assignments were established using a contribution of the two-dimensional ^1H, ^1H TOCSY, NOESY, and ROESY experiments. The $^{13}C\alpha$ signals were assigned using ^{13}C Heteronuclear Single Quantum Correlation (HSQC), ^{13}C HSQC with multiplicity editing during selection step [28, 29] and HMBC [30] experiments on a ^{13}C natural abundance sample.

2.3. NMR Spectroscopy of Ligand-Protein Interaction

The NMR sample of peptide in the presence of *β*-TrCP contained 20 μM protein (1.2 mg/ml) and 2 mM peptide, for a ratio of 100:1 peptide: protein binding sites, in Phosphate-Buffered (PB) solution, 50 mM (NaH_2PO_4/Na_2HPO_4), pH 7.2, containing 0.02% NaN_3 and 10% ^2H_2O.

After proper correction, titration WaterLOGSY permits the evaluation of the dissociation binding constant. The details of the pulse sequence version used for the WaterLOGSY experiment reported here, Fig. (**2A**) can be found in the literature [7, 31]. The first water selective 180° pulse does not require high selectivity and, in our experiment, a pulse of 20 ms length was found to be sufficient. The first two Pulsed Field Gradients (PFGs) have a typical length (2*p18) of 2 ms, Fig. (**3A**) and a power strength of 4.4 G/cm. This strength is sufficient to destroy the unwanted magnetization while avoiding signal losses due to diffusion occurring between the first two PFGs. A weak rectangular PFG is applied during the entire length of the mixing time. A short gradient recovery time of 1 ms is applied at the end of the mixing time before the detection pulse. The water suppression in both experiments was achieved with the excitation sculpting sequence [21]. The two water-selective 180° square pulses and the four PFGs of the scheme were 2.7 ms. The data were collected with a sweep width of 6009 Hz, an acquisition time of 1.4 s, and a relaxation delay of 0.5 s. Prior to Fourier transformation the data were multiplied with an exponential function with a line broadening of 1 Hz.

The one-dimensional STD-NMR [5, 8] spectrum of *β*-TrCP-peptide was performed with 1,024 scans (or 10,240 for a better signal-to-noise ratio), a relaxation delay of 2.0 s and eight dummy scans were employed to reduce subtraction artifacts as shown in Fig. (**2B**). In order to compensate for the large difference in T_2 times between the aromatic groups and the others signals [32], the irradiation was set to 0.2 to 4.0 s (Fig. (**3B**)). However, no significant results were observed for the *β*-TrCP-peptide system. Thus the irradiation time at 2 s was selected for efficient transfer of saturation from the protein to the ligand protons (Fig. (**3B**)). A series of 40 Gaussian shaped pulses (50 ms, 1 ms delay between pulses, B1/2 = 110 Hz) were used, for a total saturation time of 2.04 s. STD spectra were recorded with selective saturation of protein resonance with *on resonance* irradiation at 11 ppm and –1 ppm and *off resonance* irradiation at 30 ppm for reference spectra. To minimize the artifacts due to the irradiation at –1 ppm, the irradiations were done at 11 and –1 ppm alternately. In this case, no enhancements of the methyl signals of the peptides were observed. The 1D STD spectra were obtained by internal subtraction of saturated spectra from reference spectra by phase cycling.

2.4. Three-Dimensional Structure Calculation

The calculated distances were incorporated into a simulated annealing protocol within the program ARIA 1.2 [33, 34]. Details on the three-dimensional structure calculation were presented elsewhere [18]. PyMOL [35] was used for the analysis and presentation of the results of structure determination.

The final step of the work was a docking analysis using Surflex-Dock 2.0 (SYBYL 7.3). This sotfware is a fully flexible molecular docking algorithm that combines the scoring function of the Hammerhead docking system and a

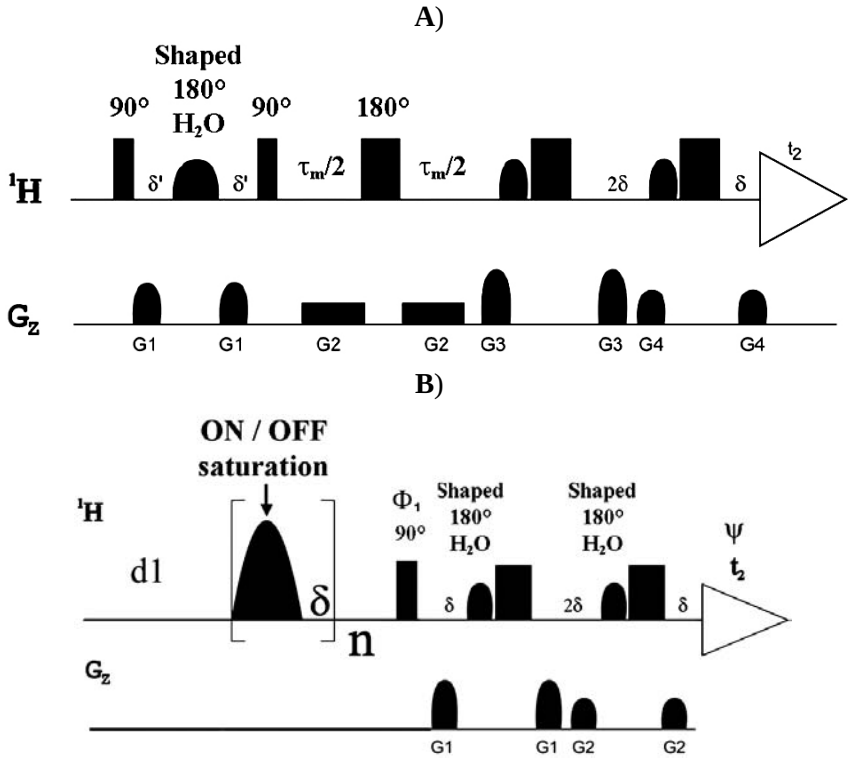

Fig. (2). Pulse sequences for homonuclear one-dimensional WaterLOGSY (upper panel) and STD (lower panel) experiments. **A**) WaterLOGSY pulse sequence. Phase cycling conditions: first water selective 180° = (*x, -y, -x, y*), and during acquisition (*x, -x, x, -x, -x, x, -x, x*). The first two PFGs have a typical length of 2 ms and a power strength of 4.4 G/cm. **B**) STD pulse sequence illustrating the saturation as a series of shaped low powered pulses just before the 90° pulse. The subtraction is performed after every scan *via* phase cycling. Phases are $\phi 1$ = *(x, -x, -x, x, y, -y,-y, y, -x, x, x, -x, -y, y, y, -y)*, and Ψ = *2 (x), 2 (-x), 2 (y), 2 (-y), 2(-x), 2(x), 2 (-y), 2(y).* The length of the selective pulse is 50 ms and the delay δ between the pulses is 1 ms, the duration of the presaturation period is adjusted by the number of pulses n (n = 40), d1 is an additional short relaxation delay (0.1 sec). d1 can be increased to better substract signal of small non-ligand during difference spectra. The intensity of the selective saturation Gauss pulses is about 110 Hz. To remove the fast relaxing protein signals, a $T_{1\rho}$ or a T2 filter can be included before acquisition. The water suppression was achieved using the excitation sculpting sequence.

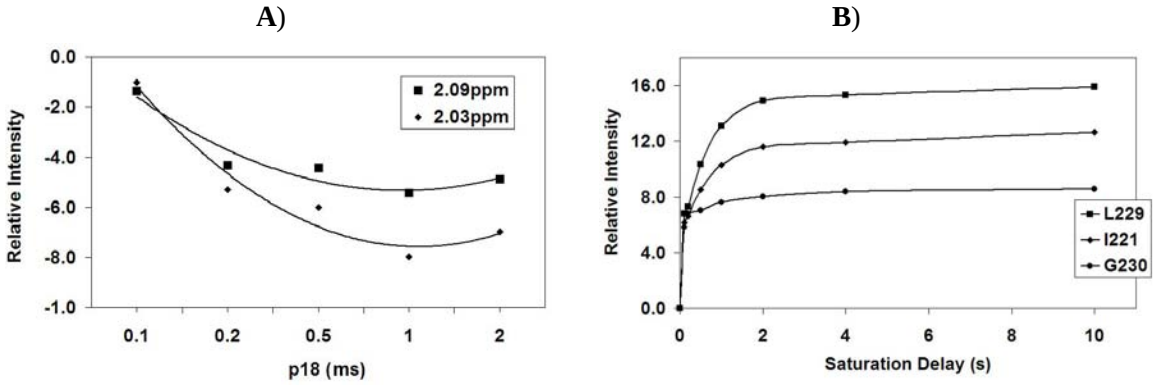

Fig. (3). A) WaterLOGSY relative intensities of two methyl signals plotted against the mixing time (2*p18). The p18 value of 1 ms was set as optimal. For the WaterLOGSY experiment, the first two Pulsed Field Gradients (PFGs) have a typical length (2*p18) of 2 ms. **B**) STD amplification factors of signals for three residues of the 23P-ATF4 peptide plotted against the saturation delay. The irradiation time at 2 s was selected for efficient transfer of saturation from the protein to the ligand protons.

patented search engine to dock ligands into a protein binding site [36]. Surflex-Dock scores are expressed in -log(K_d) units to represent binding affinities. In the first docking stage, the process started from the structure initially derived from the complex β-TrCP protein bound to a ligand β-catenin peptide, a co-crystallized molecule (PDB ID code 1P22) [14]. The protein structure consists of the three-dimensional structure of the human β-TrCP-Skp1 complex. To examine the possible mechanism of action of ligands on β-TrCP receptors, the β-catenin peptide was substituted for various

NMR peptide conformations in the β-TrCP binding site. The peptides were taken in their putative binding conformations, and were superimposed on β-catenin in the X-ray model.

3. CHARACTERIZATION OF THE COMPLEX

3.1. Biological Context

For ubiquitination, substrate proteins are recruited to the SCF E3 ubiquitin ligase complexes through interaction with the substrate-binding domain (WD-40 or leucine-rich repeats) of the F-box receptor subunits (Fig. (**1**)). SCF-β-TrCP is also responsible for phosphorylation-dependent ubiquitination and then for the degradation of IκB-α and β-catenin [37-42]. Vpu, IκB-α, and β-catenin (Table 1) share a common motif, D**pS**G*XX***pS** and phosphorylation of their serine residues are required for interaction with the β-TrCP protein [43, 44]. It is commonly thought that IκB-α is subsequently ubiquitinated and degraded in the cytoplasm, resulting in Nuclear Factor kappa B (NF-κB) nuclear translocation and transcription stimulation of target genes [45]. Similarly, it is also thought that β-catenin ubiquitination and subsequent degradation take place in the cytoplasm, preventing nuclear translocation of the protein which is required for TCF/LEF transcriptional activation of target genes [46]. This binding process plays a key role in a variety of pathological states, and has therefore been the target for numerous studies.

Moreover, in recent years, many ligands of the β-TrCP protein were discovered [47-72]. These new ligands do not always share the same common motif but are all recognized by the SCF-β-TrCP complex. One of them is ATF4 [18, 73]. Association between the two proteins depends on ATF4 phosphorylation and on ATF4 serine residue 219 present in the context of D**pS**G*XXX***pS**, which is similar but not identical to the motif found in other substrates of β-TrCP (Table 1). SCF-β-TrCP tightly modulates the stability of the transcription factor ATF4 and therefore also modulates its transcriptional activity following activation of the cAMP pathway.

Understanding the binding process between the partners is then crucial to consider the rational synthesis of specific inhibitors. Determining K_d is the starting point for characterizing the complex.

3.2. Determination of the Equilibrium Constants K_d.

3.2.1. Chemical Shifts

The dissociation constant was measured for the interaction of the phosphorylated peptides to the MBP-β-TrCP protein. The interaction caused environmental changes on the peptide protein interfaces thereby affecting the chemical shifts of the nuclei in this area. We followed the NH resonances to their bound position; the binding constant was obtained by fitting the fractional shift against an equation depending on total MBP-β-TrCP protein and peptide concentrations [74, 75]. The K_d is estimated around 2.10^{-4} M for Vpu and was characteristic of fast exchange condition, and 5.10^{-4} M for 24P-IκBα and 10^{-3} M for 32P-β-catenin respectively. The dissociation constant of 23P-ATF4 was not available because of the isomerization of the peptide.

3.2.2. WaterLOGSY

As defined by Dalvit *et al*. [7], WaterLOGSY represents a powerful method for primary NMR screening in the identification of compounds interacting with macromolecules [7] and this method is particularly useful for the evaluation of the dissociation binding constant. The WaterLOGSY method [4, 7] is based on relaxation pairs of spin neighbors. The exploited magnetization transfers are those that take place between the ligand and the solvent (the water molecules here). It is indeed shown that water, in addition to being abundant around free ligands and on hydrophilic protein surfaces, is also present in the hydrophobic cavities that ligand-protein binding sites constitute The water molecules have a relatively long time residence on hydrophobic cavities and a time correlation τ_C in the vicinity of several nanoseconds, comparable to that of macromolecule targets. This correlation time contrasts with that of water molecules in solution (a few picoseconds). This difference of dynamics is exploited in the WaterLOGSY method, which is very sensitive and easy to implement [76, 77].

Titration WaterLOGSY can be recorded to extract, after proper correction, the evaluation of K_d. However, particular care must be taken in the analysis of the titration experiments, since two offsetting effects are responsible for the signal intensity in the WaterLOGSY spectra. Both experimental points should connect on a line crossing the origin. The WaterLOGSY signals for the ligand in the presence of the protein can then be corrected by subtracting the value of the ligand signals recorded in the absence of the protein. The resulting corrected data are now related to a conventional dose-response curve and, assuming a simple binding mechanism, the data can be fitted to the equation (1):

$$I = \frac{-I_{max}}{1 + \frac{L}{K_d}} + I_{max} \quad (1)$$

where I_{max} is the maximum WaterLOGSY signal, K_d is the dissociation binding constant and L is the free ligand concentration [7]. The values for K_d measured with Equation (1) are estimated to: Vpu, K_d = 0.2 ±0.05 mM (Fig. (**4**)); 24P-IκBα, K_d = 0.6 ±0.02 mM; ATF4, K_d = 0.5 ±0.05 mM at 280 K. These K_d values are acceptable, considering the few data points required and the selectivity of the NMR experiment.

3.2.3. Fluorescence

Fluorescence experiments were performed on a Perkin-Elmer fluorometer in a 10 x 10 mm cuvette at 290 K with stirring [78]. The excitation was at 275 nm (band with 2.5 nm), and emission was recorded at 303 nm (band with 5 nm). The buffer was 50 mM sodium phosphate, pH 7.2. Since the addition of high amounts of peptides also increased the final volume by a few percentage points, a correction was introduced to take the dilution factor into account in the corresponding experiments. The determination of β-TrCP-peptide equilibrium constants (K_d) was performed (Fig. (**5**)),

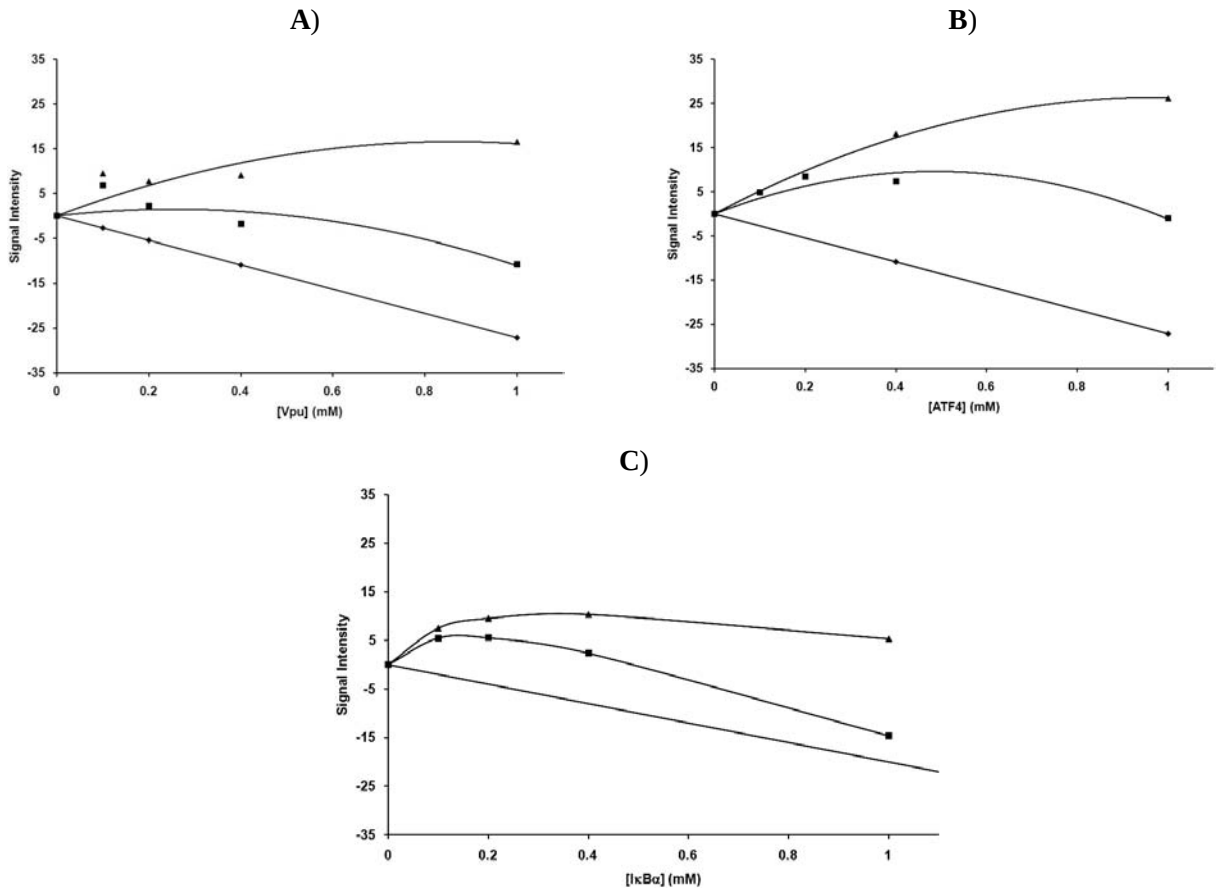

Fig. (4). Plot of WaterLOGSY signal intensities for **A**) Vpu, **B**) ATF4 and **C**) IκBα as a function of ligand concentration. The circles and diamonds are experimental points recorded in the absence and presence of 20 μM of *β*-TrCP respectively. The triangles represent the difference in intensity between the signal in the presence and absence of the protein.

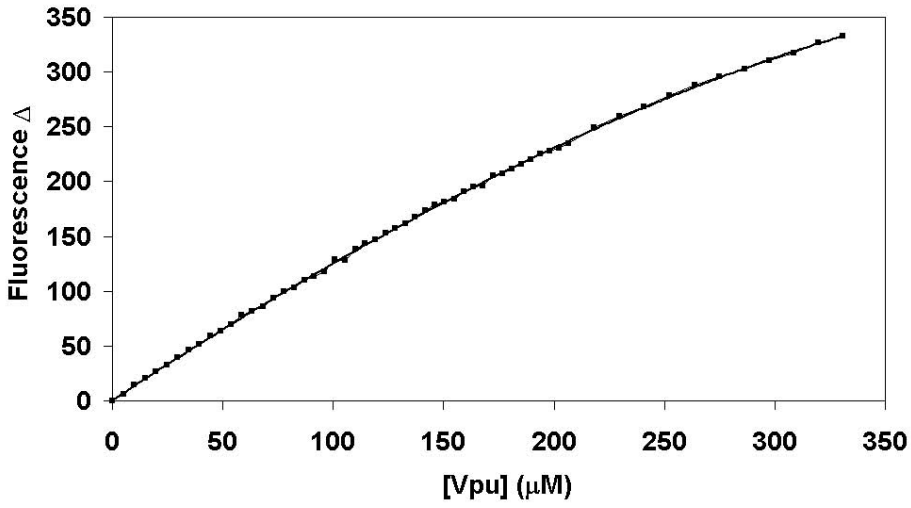

Fig. (5). Typical fluorescence results obtained with the 22P-Vpu peptide. The curves represent the relative fluorescence variation compared to the initial fluorescence of *β*-TrCP and corrected by a factor corresponding to the dilution induced by peptide addition, as a function of final peptide concentration. *β*-TrCP initial concentration was 0.1 μM. The experiment was carried out in 50 mM phosphate buffer, pH 7.2. The curve obtained has an asymptotic shape.

assuming a simple bimolecular association (Vpu, K_d = 1 mM at 290 K). Control experiments were carried out using samples where the protein MBP-*β*-TrCP was omitted.

3.2.4. Surface Plasmon Resonance

Biacore experiments were performed at 280 K and 290 K in phosphate buffer on a Biacore 2000 instrument [79]. First,

β-TrCP was covalently linked at 298 K, through its solvent-accessible primary amine groups, to the carboxymethylated dextran matrix of a CM5 sensorchip using the Amine Coupling kit (Biacore AB, Uppsala, Sweden). The samples (20-30 μL) were injected across the CM5 (*β*-TrCP) surface at concentrations ranging from 0.1 mM to 5 mM. Control experiments were performed on an empty CM5 surface. The dissociation constant, K_d, of Vpu was estimated around 6.5 mM at 280 K and was characteristic of fast exchange conditions, as depicted in Fig. (**6**). At 290 K, no significant results were obtained.

No significant differences in the calculated dissociation rate either by fluorescence or with the Biacore apparatus were observed for Vpu peptide, even though these experiments were carried out at different temperatures.

In conclusion, these results allow us to classify the different ligands based on their affinity for the *β*-TrCP. The Vpu peptide is the best of the four ligands. The second best ligand appears to be 23P-ATF4, followed by the 24P-IκBα peptide, the 32P-*β*-catenin peptide coming last. These results are in agreement with those obtained by Besnard-Guerin *et al*. [44]. In this paper, they show that Vpu prevented the proteosomal degradation of the *β*-catenin, IκB-α and ATF4 protein. They also show that the overexpression of ATF4 provoked accumulation of *β*-catenin. Our results are consistent with their conclusions.

3.3. Epitope Mapping

After investigating the conformational preferences of peptides when free in solution, we set out to investigate their interactions with the *β*-TrCP protein. Therefore, STD [5, 8, 9, 80, 81] and TRNOE [82, 83] NMR experiments were performed. The NMR sample of peptide in the presence of *β*-TrCP contained 20 μM protein (1.2 mg/ml) and 2 mM peptide, for a ratio of 100:1 peptide: protein binding sites.

The STD-NMR technique allows to determine the binding area of ligands also called "epitope mapping" by NMR spectroscopy. It can be combined with any NMR pulse sequence, which is a sizeable advantage. Moreover, in the 1D mode, the method is fast and reliable (Fig. (**2B**)) [5]. This experiment is carried out with a large excess of ligand. The spectrum of the macromolecule is saturated by selective irradiation in a spectral range that does not contain ligand resonances. During the experiment, resonances of the protein are selectively saturated, spin diffusion in the macromolecule allows the transfer of saturation (*via* intramolecular NOEs) and finally, ligand-protein intermolecular NOE allows the transfer of saturation to the ligand. These negative NOE effects may be observed as enhancements in the difference (STD-NMR) spectrum resulting from subtraction of this spectrum from a reference spectrum in which the protein is not saturated. The only signals present were those resulting from the transfer of saturation from bound to free ligand, thus allowing their immediate identification. Enhancements are mainly observed for the resonance of protons in close contact with the protein. STD allows direct observation of areas of the ligand that comprise the epitope [5, 8, 9, 80, 81].

The individual signal protons of the peptide are better analyzed from the intensity values than the integral values in the reference (I_0) and STD spectra ($I_{STD}=I_0-I_{sat}$). The spectral region corresponding to the amino protons is well resolved and can be used to classify the amino acid residues relevant for interaction with the protein, for example the IκB-α peptide in interaction with *β*-TrCP (Fig. (**7**)). The moderate degree of overlapping for the amide protons allowed us to calculate the intensity for all the visible amide protons of the

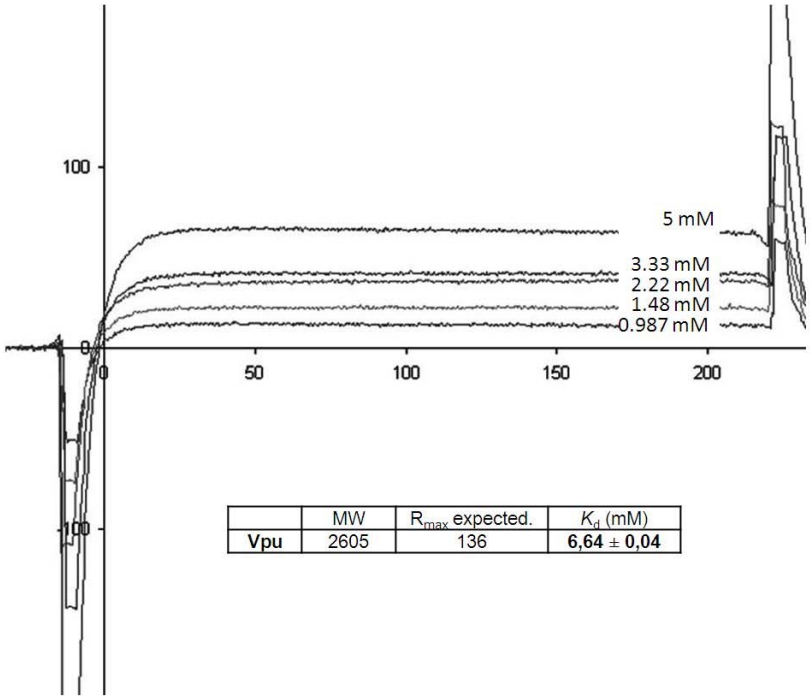

	MW	R_{max} expected.	K_d (mM)
Vpu	2605	136	**6,64 ± 0,04**

Fig. (6). Surface Plasmon Resonance (SPR) analysis of binding activity of Vpu to *β*-TrCP. All curves are obtained after blank subtraction.

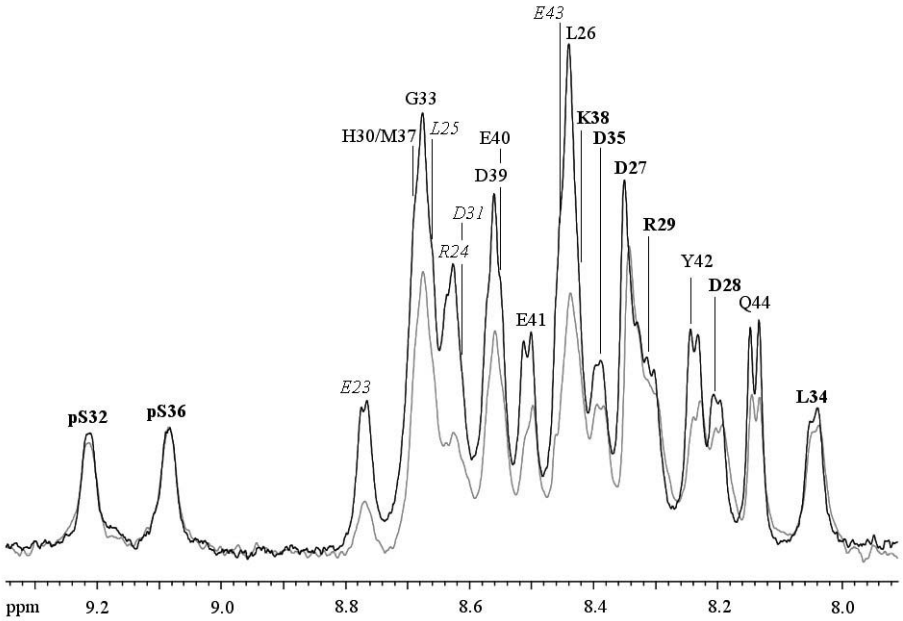

Fig. (7). Region containing resonances of the amide protons of the 24P-IκBα peptide in association with the *β*-TrCP protein. Reference 1D ^{1}H spectrum (in black) and 1D ^{1}H STD-NMR spectrum (in light grey), showing enhancements of resonances of protons making close contacts with protein interaction sites.

peptide. The signal obtained with the largest I_{STD}/I_0 value, was normalized to 100% (Fig. (**8**)). The relative degree of saturation for the individual protons, normalized to that of the maximum intensity, can be used to compare the STD effect [8].

The STD spectrum of the 22P-Vpu peptide clearly demonstrated the involvement of the NH of residues such as Leu^{45}, Ile^{46}, pSer^{52}, Gly^{53}, pSer^{56} and Glu^{57}, which have similar larger STD intensities, ranging from 70% to 100% (Fig. (**8A**)). This high saturation transfer indicated the proximity of these protons to the protein surface. Two groups of residues seem to be important for binding as they are found closer to the protein surface than the other protons. The first group is composed of residues of the D**S**G*XX***S** motif (without N54 and E55) and the second group belongs to the upstream 45-46 region.

For the 23P-ATF4 peptide, the STD spectrum shows that the whole D**S**G*XXX***S** motif is implied in the interaction with the *β*-TrCP protein. Each residue in the motif seems to be strongly and equally implied in the binding to the macromolecule. Thus, the residues Asp^{218}, pSer^{219} and pSer^{224} are the most implicated in the interaction to *β*-TrCP. The presence of the additional residue in the motif causes the 23P-ATF4 peptide to bend so as to fit the interaction site. This entails additional contacts with the *β*-TrCP protein (Fig. (**8B**)).

The 24P-IκBα peptide forms two specific contact zones. The first one is the residues of the consensus motif, without Asp^{31} and Gly^{33}, but including Lys^{38}. The second area includes residues from Asp^{26} to Arg^{29} (Fig. (**8C**)).

For the 32P-*β*-catenin peptide, the STD spectrum shows that two regions are involved in the interaction to the *β*-TrCP protein. The first part of the D**S**G*XX***S** motif, Asp^{32} to Ile^{35}, including Leu^{31}, is strongly involved in the interaction. The rest of the motif seems to be less implied in the binding. The second phosphoserine appears to have an STD intensity of around 50%. Two residues, Trp^{25} and Gln^{26}, are also involved in the binding to *β*-TrCP (Fig. (**8D**)).

For reference, the STD-NMR spectrum was recorded with samples containing the nonphosphorylated peptide, and all signals from nonbinding peptide were completely eliminated.

One of the major advantages of the technique is that the STD protocol may be combined with any NMR pulse sequence generating over 2D STD-NMR experiments such as STD TOCSY or STD HSQC [5, 80, 81]. Optimization of the STD-HSQC experiment permits to enhance the sensitivity of Cα-Hα correlations. This was obtained by subtraction of the on- and off-resonance spectra made by phase cycling [16].

Fig. (**9A**) shows a zoom region of the HSQC spectrum and Fig. (**9B**) shows the same region on the STD-HSQC spectrum for the 32P-*β*-catenin peptide. Again, we could observe how signals corresponding to residues in a close proximity to the receptor are saturated to a higher degree, resulting in more intense cross-peaks. The analysis of the relative 2D STD-HSQC volumes of 32P-*β*-catenin was also accomplished by integrating the cross-peaks and referencing them to the most intensive proton signals, as we did for the 1D STD analyses. The cross-peaks corresponding to Leu^{31}, Ile^{35} and Ala^{39} are present in the spectrum Fig. (**9B**), which means that the aforesaid residues interact with the *β*-TrCP protein. Conversely, it is interesting to notice that signals from Ala^{21}, Val^{22}, and Leu^{46} present in the HSQC spectrum (Fig. (**9A**)) have nearly all disappeared in the STD-HSQC

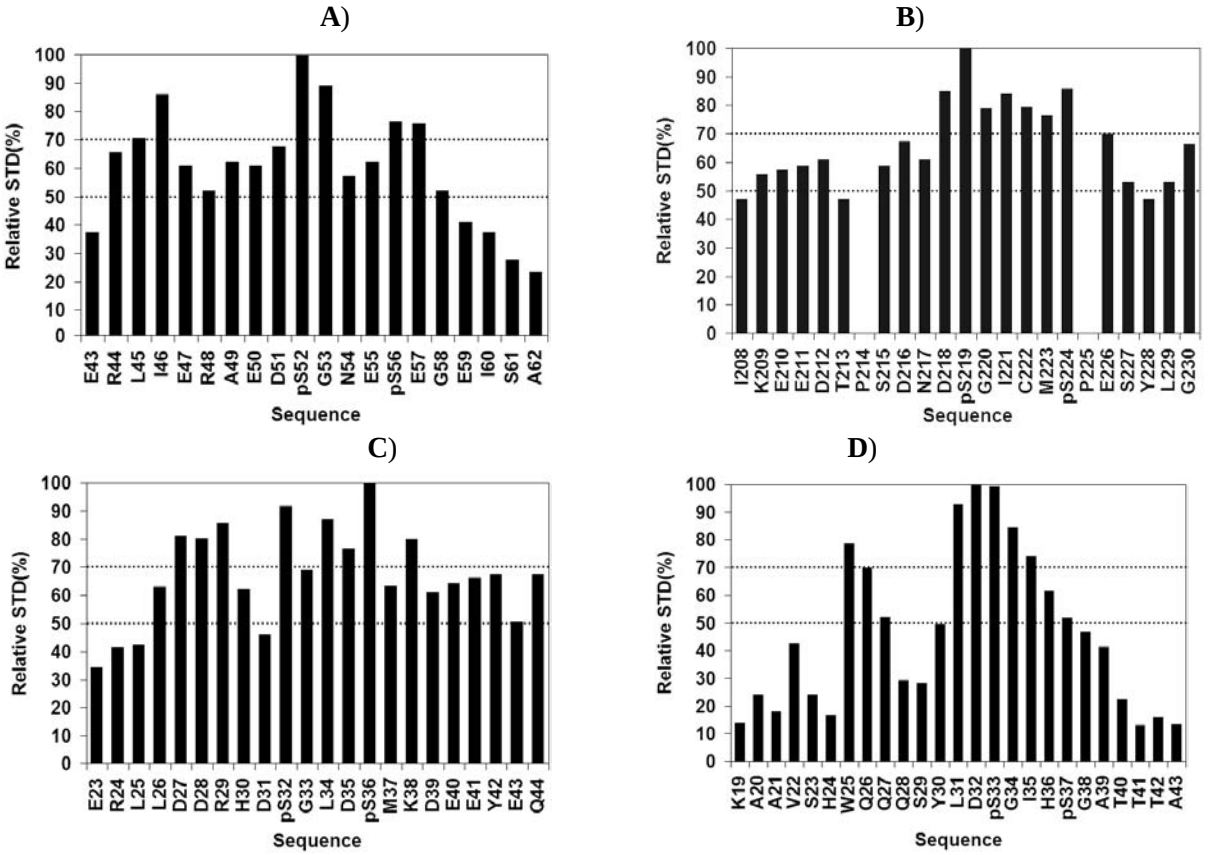

Fig. (8). Relative STD intensities (in percent) of the amide protons of the individual amino acids calculated for each amino acid of the different peptides from the 1D spectrum. **A**) Relative STD for the 22P-Vpu peptide. There are two areas, upstream from the D**pS**G*XX***pS** motif (L45-I46), and the residues of the D**pS**G*XX***pS** motif. **B**) For the 23P-ATF4 peptide, only the consensus motif seems to be strongly implied in the interaction. **C**) For the 24P-IκBα peptide, two areas appear, one upstream from the motif (D27-R29) and one including the motif containing the two phosphoserines. **D**) For the 32P-*β*-catenin peptide, there are two areas, before the motif (W25-Q26) and around the first phosphoserine.

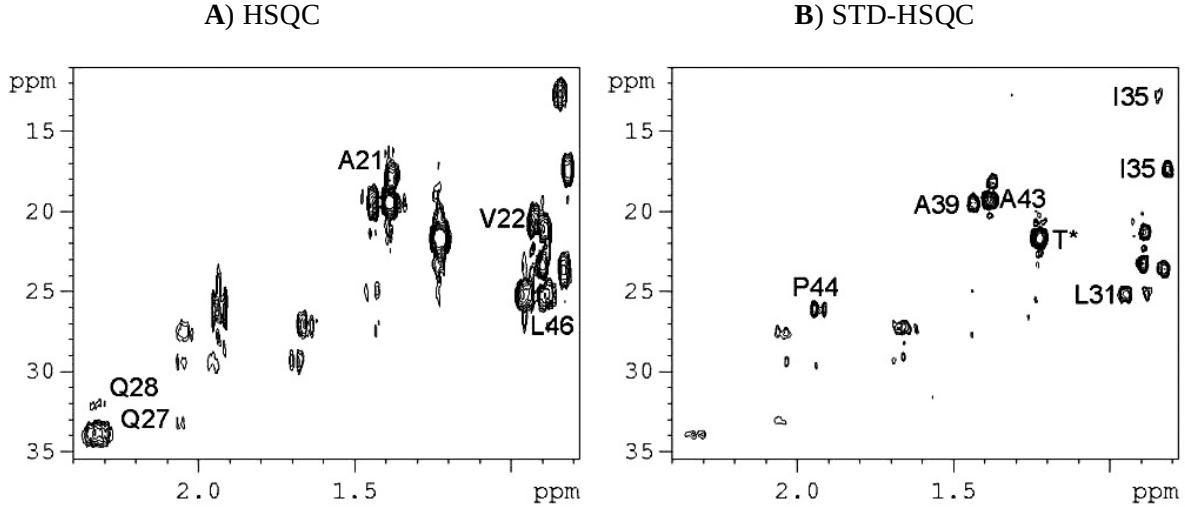

Fig. (9). **A**) 2D ^{1}H-^{13}C HSQC region of the complex 32P-*β*-catenin/*β*-TrCP protein. **B**) Corresponding 2D STD HSQC region spectrum. Ala21 and Val22 show low intensity signals in the STD-HSQC experiment. Other strong signals are identified with the one letter amino acid code. Threonine residues 40, 41 and 42 are identified with an asterisk, because resonances overlap [16].

spectrum (Fig. (**9B)**) because of their low degree of saturation. To summarize, when the signals in the 1D spectrum are not resolved enough, the binding epitope could be determined from 2D cross-peak integrals.

Surprisingly, signals of the Hγ of Gln^{27} and Gln^{28} are weak in the STD-HSQC spectrum, whereas their HN were quite strong in the 1D STD spectrum. These additional contacts are also present in the Vpu and IκB-α peptides but they implied different kinds of residues (hydrophobic, polar and charged). These contacts are relatively intense (STD intensity of around 80%). But to a large extent, the results are in agreement with those of the 1D STD experiment.

3.4. Peptide Structures

If binding is sufficiently weak to allow exchange (fast on the time scale of spin-lattice relaxation rate), the TRNOEs NMR experiment is well adapted to study the bound conformation in a ligand-receptor complex transferred to the free molecule *via* chemical exchange.

The combination of STD-NMR epitope mapping data with knowledge of the bound conformations of ligands, which may be obtained by transferred nuclear Overhauser effect spectroscopy (TRNOESY) experiments, is a powerful method to build up models of protein-ligand interaction [84-86]. Therefore, TRNOESY experiments [82, 83] were used to investigate the bound conformation of the peptide. The optimal conditions for the TRNOESY measurements were determined by considering a peptide: β-TrCP molar ratio of 100 with mixing times (τ_m) of 50, 100, 200, 300 and 500 ms.

Faster rate of build-up for the peptide in presence of β-TrCP was observed (Fig. (**10**)), which indicated the binding of the peptide to the β-TrCP protein. The observation of supplementary TRNOE cross-peaks after the macromolecule was added demonstrates the peptide–protein interaction. Significant differences were observed between the NOESY spectra of the free peptide and that of the peptide bound to the β-TrCP protein, indicating that the cross-peaks observed in presence of the β-TrCP protein are in fact TRNOEs. The build-up curve [87] for different NOE correlations showed that spin diffusion was negligible for a τ_m of 150 ms (Fig. (**10**)).

TRNOEs experiments lead to distant restraints. The final list of constraints was incorporated for structure calculation with the standard protocol of ARIA 1.2 [34, 88]. The NMR bound structures of the peptides in interaction with the β-TrCP protein were then used in docking. As described in Materials and Methods, ligand flexibility was treated by pre-generating bound ligand conformers with the ARIA software and then docking each bound ligand conformer into the protein target as a rigid molecule.

3.5. Docking of the NMR Structures

We have knowledge of the structure of the bound peptide, yet the binding mode of the peptide to the target remains unknown. To view the complex, it is necessary to conduct the docking of the NMR structures with the crystallographic structure of the protein β-TrCP. Indeed, no other crystal structure has been discovered in interaction with a ligand since 2003 [14]. It is the only way for us to see the interaction.

The β-TrCP binding site is formed by a channel running through the middle of the WD40 β propeller structure with a hydrophobic pocket and positively charged residues at the top face of the β propeller, thus presenting potential locations for hydrogen bonds to the peptide ligand. For docking calculations, the ligand was placed near this putative binding site. The docking routine generated randomized ligand - β-TrCP protein assemblies using the Surflex-Dock program. The β-TrCP protein was capted rigid and peptides were flexible. This allowed sampling of the conformational space toward induced fit shapes. Approximations were introduced into the docking routine by defining the length of the peptide backbone NMR and by fixing the β-TrCP protein framework. However, each of the most frequently found complex geometries reflected a putative conformation and

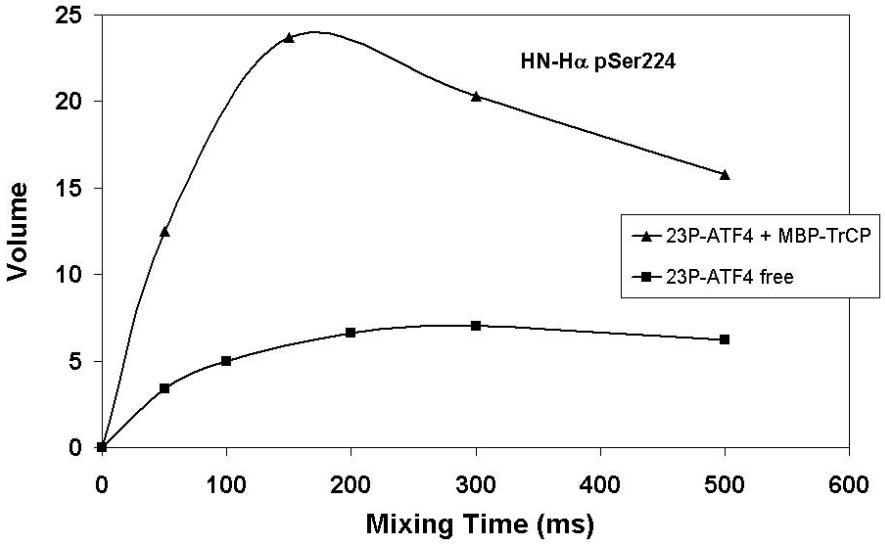

Fig. (10). TRNOE build-up rates of 23P-ATF4 peptide with and without β-TrCP vs. mixing time (ms). The ligand to β-TrCP ratio is 100:1. The curves represent the intra-residue connectivity HN-Hα of pSer224.

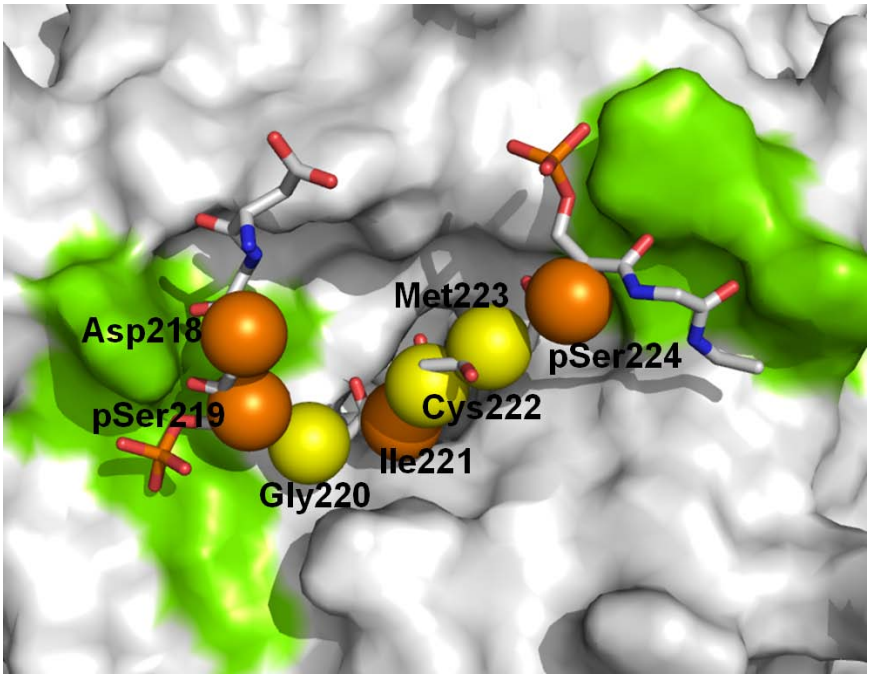

Fig. (11). Docked structures of ATF4 starting from the NMR bound structure. The surface representation of the top face of the β-TrCP WD40 domain with the bound D**pS**G*XX***pS** motif, highlighted two interaction sites (Tyr^{271}, Arg^{285}, Ser^{309}, Ser^{325} and Arg^{410}, Arg^{431}, Gly^{432}, Ser^{448}). STD results have been added to the structure. The amide protons with the strongest STD amplification factor are displayed as *colored spheres*: *orange* for the strongest values, Asp^{218}, Ile^{221}, **pSer**^{219} and **pSer**^{224}; *yellow* for intermediate values, Gly^{220}, Cys^{222}, Met^{223} and Glu^{226}.

the ultimately selected one was in accordance with experimental NMR bound structure.

The phosphorylated ligands were then cross-docked into the β-TrCP crystal structure originally bound with the 11P-β-catenin peptide *via* their bound structures obtained by minimization under NMR constraints. The phosphoserine, aspartic acid, and hydrophobic residues of the motif were recognized directly by β-TrCP, as shown in Fig. (**11**).

All seven WD40 repeats of β-TrCP contribute to interact with the different ligands. We can generally determine main common parts of the different ligands in contact with three β-TrCP binding pockets. The W1-W2 β-TrCP binding domain is common for all the ligands. Important contacts with the W4-W5 domain are observed for β-catenin, IκB-α and ATF4. Moreover, β-catenin and IκB-α have supplementary contacts with the W6-W7. Vpu has very specific interactions with the β-TrCP. Indeed Vpu interacts with the W5-W6 region making hydrogen bonds and the five aspartic and glutamic acid residues imply an overall negative potential and provide a putative binding region. Thus, the strongest interactions are mainly electrostatic interactions with the W3 domain.

3.6. STD Binding Competition

A great number of substrates of β-TrCP have been identified up to now. All of them share similar although not identical phosphorylation destruction motifs compared to the canonical D**S**G*XX***S** motif identified in the first known substrates of β-TrCP. All of these substrates bind to the seven WD domain of β-TrCP only if they are phosphorylated on the serine residues of this motif, with a more important role devoted to the first Ser residue. To understand the mechanism of action of β-TrCP and the importance of its functions in regulating numerous cellular pathways, it is crucial to determine whether and how all these substrates are able to compete between each other for binding to the same domain of β-TrCP. It will help considerably to modulate the activity of β-TrCP for therapeutic purposes against cancer and inflammation processes for example, while avoiding undesirable side effects due to other non-targeted substrates. Toward this goal, we were able to analyze by STD-competition experiment the behavior of two different substrates with respect to β-TrCP when both were simultaneously present with the receptor E3 ligase protein. Thus, it could demonstrate that ATF4 was in competition with β-catenin for binding to β-TrCP. Hence, this STD-competition approach will pave the way for experimental design intended to specifically modulate a particular substrate of β-TrCP while avoiding to inhibit another non-targeted substrate.

This experiment allows the detection of the weak active site ligand, *i.e.* β-catenin compared to the higher-affinity ligand *i.e.* ATF4 (Fig. (**12**)). ATF4 seems to be a better ligand (K_d around 0.5 mM) of the β-TrCP protein than β-catenin (K_d around 1 mM). The ability to determine the binding affinity of inhibitors by the competition STD-NMR method leads to a rapid rank ordering of potential inhibitors that involves the evaluation of large numbers of analogs.

4. CONCLUSION AND OUTLOOK

NMR is now being recognized by industry experts as a powerful technique for lead discovery [89]. Although its principles were essentially discovered and developed long

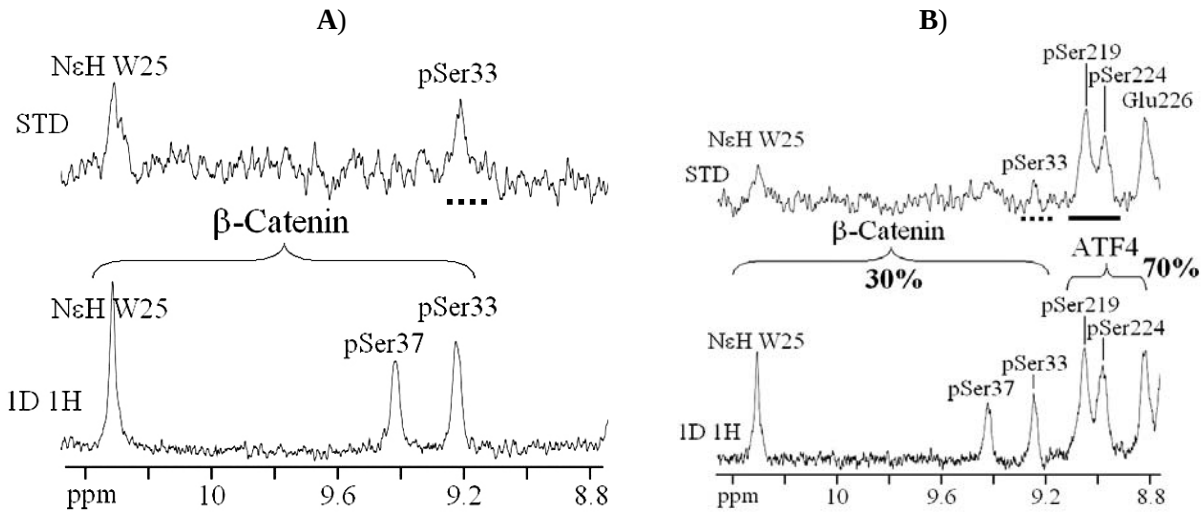

Fig. (12). Competition STD-NMR. The 1D proton and STD-NMR spectra of 32P-*β*-catenin/*β*-TrCP upon addition of 23P-ATF4 illustrates the STD signal reduction of the indicator (32P-*β*-catenin) as a function of the competitor (23P-ATF4) concentration at different P-*β*-catenin:P-ATF4 ratios. **A**) 1D proton spectrum of a weak ligand, 32P-*β*-catenin ($K_d \approx 1$ mM) used as an STD indicator at a concentration of 0.4 mM in the presence of 20 μM *β*-TrCP protein. Residues **pSer**^{33}, and the aromatic protons NεH of Trp^{25} in close contact with *β*-TrCP protein, show positive peak in the STD-NMR spectrum. **B**) Upon addition of the 23P-ATF4 peptide (30:70). The 1D proton and STD-NMR spectra of the same sample show that the STD signal intensities of 32P-*β*-catenin were reduced whereas the STD signal of the **pSer**^{219}**,** **pSer**^{224}**,** and Glu^{226}**,** amide signals of 23P-ATF4 at 9.05, 8.90 and 8.79 ppm, respectively were increased.

ago, there are numerous novel applications. The protein-protein interactions can be efficiently detected using this novel NMR reporter system. Its primary advantage is the characteristic of indirect detection, due to which only minute amounts of protein material and no isotope labeling are required. We have offered a range of the available NMR methods and outlined possible future developments by a reduction to basic NMR properties and principles. These techniques nevertheless have clear advantages for pre-screening large libraries as they implicitly deconvolute ligand mixtures, require no isotope labelling and pose few limitations on the target.

In this mini review, a number of examples were presented that demonstrate the scope of NMR methods to identify and characterize the binding of ligands to receptor proteins. With these methods, one can sort out molecules that bind to the target from those that do not. Using WaterLOGSY or line broadening, the dissociation constant is easily determined. The STD-NMR technique allows to determine atoms in close contact with the target and to define an epitope mapping of the binding site. The TRNOESY experiments permit to characterize the NMR bound structure. Using a powerful docking process, one can precisely determine the location of the binding site and the binding mode of two proteins.

ACKNOWLEDGEMENTS

We would like to gratefully thank Patrick England and Sylviane Hoos for their help with the Biacore instrument and Michel Vidal for his help with the fluorescence experiments. We thank Julie Lecas (Centre for Technical Languages, University Paris Descartes). Julien Pons was supported by a studentship from the Ministère de l'Enseignement Supérieur et de la Recherche.

This work was supported by grants from the Ministère de l'Enseignement Supérieur et de la Recherche, and the Agence nationale de recherches sur le SIDA et les hépatites virales (ANRS).

ABBREVIATIONS

ATF4	=	Activating transcription factor 4
β-TrCP	=	*β*-Transducin repeat containing protein
HSQC	=	Heteronuclear single quantum correlation
IκB-α	=	Inhibitor of nuclear factor kappa B alpha
MBP	=	Maltose binding protein
NOESY	=	Nuclear overhauser effect spectroscopy
ROESY	=	Rotating-frame overhauser enhancement spectroscopy
SCF	=	Skp1-Cullin-FBox
Skp1	=	Suppressor of kinetochore protein
STD	=	Saturation transfer difference
TOCSY	=	Total correlation spectroscopy
TRNOESY	=	Transferred nuclear overhauser effect spectroscopy
WaterLOGSY	=	Water ligand observed *via* gradient spectroscopy

REFERENCES

[1] Shuker, S.B.; Hajduk, P.J.; Meadows, R.P.; Fesik, S.W. Discovering high-affinity ligands for proteins: SAR by NMR, *Science*, **1996**, *274*, 1531-4.

[2] Chen, A.; Shapiro, M.J. NOE pumping: A novel NMR technique for identification of compounds with binding affinity to macromolecules, *J. Am. Chem. Soc.*, **1998**, *120*, 10258-59.

[3] Chen, A.; Shapiro, M.J. NOE pumping. 2. A high-throughput method to determine compounds with binding affinity to macromolecules by NMR, *J. Am. Chem. Soc.*, **2000**, *122*, 414-15.

[4] Dalvit, C.; Pevarello, P.; Tato, M.; Veronesi, M.; Vulpetti, A.; Sundstrom, M. Identification of compounds with binding affinity to proteins *via* magnetization transfer from bulk water, *J. Biomol. NMR*, **2000**, *18*, 65-8.

[5] Mayer, M.; Meyer, B. Characterization of ligand binding by saturation transfer difference NMR spectroscopy, *Angew. Chem. Int. Ed. Engl.*, **1999**, *38*, 1784-88.

[6] Bertho, G.; Gharbi-Benarous, J.; Delaforge, M.; Girault, J.P. Transferred nuclear Overhauser effect study of macrolide-ribosome interactions: correlation between antibiotic activities and bound conformations, *Bioorg. Med. Chem.*, **1998**, *6*, 209-21.

[7] Dalvit, C.; Fogliatto, G.; Stewart, A.; Veronesi, M.; Stockman, B. WaterLOGSY as a method for primary NMR screening: practical aspects and range of applicability, *J. Biomol. NMR*, **2001**, *21*, 349-59.

[8] Mayer, M.; Meyer, B. Group epitope mapping by saturation transfer difference NMR to identify segments of a ligand in direct contact with a protein receptor, *J. Am. Chem. Soc.*, **2001**, *123*, 6108-17.

[9] Klein, J.; Meinecke, R.; Mayer, M.; Meyer, B. Detecting binding affinity to immobilized receptor proteins in compound libraries by HR-MAS STD NMR, *J. Am. Chem. Soc.*, **1999**, *121*, 5336-37.

[10] Wang, Y.S.; Liu, D.; Wyss, D.F. Competition STD NMR for the detection of high-affinity ligands and NMR-based screening, *Magn. Reson. Chem.*, **2004**, *42*, 485-9.

[11] Ciechanover, A. The ubiquitin-proteasome pathway: on protein death and cell life, *EMBO J.*, **1998**, *17*, 7151-60.

[12] Hershko, A.; Ciechanover, A. The ubiquitin system, *Annu. Rev. Biochem.*, **1998**, *67*, 425-79.

[13] Laney, J.D.; Hochstrasser, M. Substrate targeting in the ubiquitin system, *Cell*, **1999**, *97*, 427-30.

[14] Wu, G.; Xu, G.; Schulman, B.A.; Jeffrey, P.D.; Harper, J.W.; Pavletich, N.P. Structure of a beta-TrCP1-Skp1-beta-catenin complex: destruction motif binding and lysine specificity of the SCF(beta-TrCP1) ubiquitin ligase, *Mol. Cell*, **2003**, *11*, 1445-56.

[15] Coadou, G.; Gharbi-Benarous, J.; Megy, S.; Bertho, G.; Evrard-Todeschi, N.; Segeral, E.; Benarous, R.; Girault, J.P. NMR studies of the phosphorylation motif of the HIV-1 protein Vpu bound to the F-box protein beta-TrCP, *Biochemistry*, **2003**, *42*, 14741-51.

[16] Megy, S.; Bertho, G.; Gharbi-Benarous, J.; Evrard-Todeschi, N.; Coadou, G.; Segeral, E.; Iehle, C.; Quemeneur, E.; Benarous, R.; Girault, J.P. STD and TRNOESY NMR studies on the conformation of the oncogenic protein beta-catenin containing the phosphorylated motif DpSGXXpS bound to the beta-TrCP protein, *J. Biol. Chem.*, **2005**, *280*, 29107-16.

[17] Pons, J.; Evrard-Todeschi, N.; Bertho, G.; Gharbi-Benarous, J.; Sonois, V.; Benarous, R.; Girault, J.P. Structural studies on 24P-IkappaBalpha peptide derived from a human IkappaB-alpha protein related to the inhibition of the activity of the transcription factor NF-kappaB, *Biochemistry*, **2007**, *46*, 2958-72.

[18] Pons, J.; Evrard-Todeschi, N.; Bertho, G.; Gharbi-Benarous, J.; Tanchou, V.; Benarous, R.; Girault, J.P. Transfer-NMR and docking studies identify the binding of the peptide derived from activating transcription factor 4 to protein ubiquitin ligase beta-TrCP. Competition STD-NMR with beta-catenin, *Biochemistry*, **2008**, *47*, 14-29.

[19] Nallamsetty, S.; Austin, B.P.; Penrose, K.J.; Waugh, D.S. Gateway vectors for the production of combinatorially-tagged His6-MBP fusion proteins in the cytoplasm and periplasm of Escherichia coli, *Protein Sci.*, **2005**, *14*, 2964-71.

[20] Marion, D.; Ikura, M.; Tschudin, R.; Bax, A. Rapid recording of 2D NMR spectra without phase cycling. Application to the study of hydrogen exchange in proteins, *J. Magn. Reson.*, **1989**, *85*, 393-99.

[21] Hwang, T.-L.; Shaka, A.J. Water suppression that works. Excitation sculpting using arbitrary waveforms and pulsed field gradients, *J. Magn. Reson.*, **1995**, *112*, 275-79.

[22] Piotto, M.; Saudek, V.; Sklenar, V. Gradient-tailored excitation for single-quantum NMR spectroscopy of aqueous solutions, *J. Biomol. NMR*, **1992**, *2*, 661-5.

[23] Xia, Y.; Legge, G.; Jun, K.Y.; Qi, Y.; Lee, H.; Gao, X. IP-COSY, a totally in-phase and sensitive COSY experiment, *Magn. Reson. Chem.*, **2005**, *43*, 372-9.

[24] Braunschweiler, L.; Ernst, R.R. Coherence Transfer by Isotropic Mixing: Application to Proton Correlation Spectroscopy, *J. Magn. Reson.*, **1983**, *53*, 521-28.

[25] Kumar, A.; Ernst, R.R.; Wuthrich, K. A two-dimensional nuclear Overhauser enhancement (2D NOE) experiment for the elucidation of complete proton-proton cross-relaxation networks in biological macromolecules, *Biochem. Biophys. Res. Commun.*, **1980**, *95*, 1-6.

[26] Bothner-By, A.A.; Stevens, R.L.; Lee, J.T.; Warren, C.D.; Jeanloz, R.W. Structure determination of a tetrasaccharide: Transient nuclear Overhauser effects in the rotating frame, *J. Am. Chem. Soc.*, **1984**, *106*, 811-13.

[27] Bax, A.; Davis, D.G. MLEV-17-based two-dimensional homonuclear magnetization transfer spectroscopy, *J. Magn. Reson.*, **1985**, *65*, 355-60.

[28] Bodenhausen, G.; Ruben, D.J. Natural Abundance Nitrogen-15 NMR by Enhanced Heteronuclear Spectroscopy, *Chem. Phys. Lett.*, **1980**, *69*, 185-86.

[29] Willker, W.; Leibfritz, D.; Kerssebaum, R.; Bermel, W. Gradient Selection in Inverse Heteronuclear Correlation Spectroscopy, *Magn. Reson. Chem.*, **1993**, *31*, 287-92.

[30] Bax, A.; Summers, M.F. 1H and 13C Assignments from Sensitivity-Enhanced Detection of Heteronuclear Multiple-Bond Connectivity by 2D Multiple Quantum NMR, *J. Am. Chem. Soc.*, **1986**, *108*, 2093-94.

[31] Shimotakahara, S.; Furihata, K.; Tashiro, M. Application of NMR screening techniques for observing ligand binding with a protein receptor, *Magn. Reson. Chem.*, **2005**, *43*, 69-72.

[32] Milton, M.J.; Thomas Williamson, R.; Koehn, F.E. Mapping the bound conformation and protein interactions of microtubule destabilizing peptides by STD-NMR spectroscopy, *Bioorg. Med. Chem. Lett.*, **2006**, *16*, 4279-82.

[33] Brunger, A.T.; Adams, P.D.; Clore, G.M.; DeLano, W.L.; Gros, P.; Grosse-Kunstleve, R.W.; Jiang, J.S.; Kuszewski, J.; Nilges, M.; Pannu, N.S.; Read, R.J.; Rice, L.M.; Simonson, T.; Warren, G.L. Crystallography & NMR system: A new software suite for macromolecular structure determination, *Acta. Crystallogr. D. Biol. Crystallogr.*, **1998**, *54*, 905-21.

[34] Linge, J.P.; Habeck, M.; Rieping, W.; Nilges, M. ARIA: automated NOE assignment and NMR structure calculation, *Bioinformatics*, **2003**, *19*, 315-6.

[35] DeLano, W.L. The PyMOL Molecular Graphics System, on World Wide Web http://www.pymol.org, **2002**.

[36] Jain, A.N. Surflex: fully automatic flexible molecular docking using a molecular similarity-based search engine, *J. Med. Chem.*, **2003**, *46*, 499-511.

[37] Hart, M.; Concordet, J.P.; Lassot, I.; Albert, I.; del los Santos, R.; Durand, H.; Perret, C.; Rubinfeld, B.; Margottin, F.; Benarous, R.; Polakis, P. The F-box protein beta-TrCP associates with phosphorylated beta-catenin and regulates its activity in the cell, *Curr. Biol.*, **1999**, *9*, 207-10.

[38] Kroll, M.; Margottin, F.; Kohl, A.; Renard, P.; Durand, H.; Concordet, J.P.; Bachelerie, F.; Arenzana-Seisdedos, F.; Benarous, R. Inducible degradation of IkappaBalpha by the proteasome requires interaction with the F-box protein h-betaTrCP, *J. Biol. Chem.*, **1999**, *274*, 7941-5.

[39] Latres, E.; Chiaur, D.S.; Pagano, M. The human F box protein beta-Trcp associates with the Cul1/Skp1 complex and regulates the stability of beta-catenin, *Oncogene*, **1999**, *18*, 849-54.

[40] Spencer, E.; Jiang, J.; Chen, Z.J. Signal-induced ubiquitination of IkappaBalpha by the F-box protein Slimb/beta-TrCP, *Genes Dev.*, **1999**, *13*, 284-94.

[41] Winston, J.T.; Strack, P.; Beer-Romero, P.; Chu, C.Y.; Elledge, S.J.; Harper, J.W. The SCFbeta-TRCP-ubiquitin ligase complex associates specifically with phosphorylated destruction motifs in IkappaBalpha and beta-catenin and stimulates IkappaBalpha ubiquitination *in vitro*, *Genes Dev.*, **1999**, *13*, 270-83.

[42] Yaron, A.; Hatzubai, A.; Davis, M.; Lavon, I.; Amit, S.; Manning, A.M.; Andersen, J.S.; Mann, M.; Mercurio, F.; Ben-Neriah, Y. Identification of the receptor component of the IkappaBalpha-ubiquitin ligase, *Nature*, **1998**, *396*, 590-4.

[43] Margottin, F.; Bour, S.P.; Durand, H.; Selig, L.; Benichou, S.; Richard, V.; Thomas, D.; Strebel, K.; Benarous, R. A novel human

WD protein, h-beta TrCp, that interacts with HIV-1 Vpu connects CD4 to the ER degradation pathway through an F-box motif, *Mol. Cell*, **1998**, *1*, 565-74.

[44] Besnard-Guerin, C.; Belaidouni, N.; Lassot, I.; Segeral, E.; Jobart, A.; Marchal, C.; Benarous, R. HIV-1 Vpu sequesters beta-transducin repeat-containing protein (betaTrCP) in the cytoplasm and provokes the accumulation of beta-catenin and other SCFbetaTrCP substrates, *J. Biol. Chem.*, **2004**, *279*, 788-95.

[45] Karin, M. How NF-kappaB is activated: the role of the IkappaB kinase (IKK) complex, *Oncogene*, **1999**, *18*, 6867-74.

[46] Peifer, M.; Polakis, P. Wnt signaling in oncogenesis and embryogenesis--a look outside the nucleus, *Science*, **2000**, *287*, 1606-9.

[47] Zhu, Z.; Kirschner, M. Regulated proteolysis of Xom mediates dorsoventral pattern formation during early Xenopus development, *Dev. Cell*, **2002**, *3*, 557-68.

[48] Margottin-Goguet, F.; Hsu, J.Y.; Loktev, A.; Hsieh, H.M.; Reimann, J.D.; Jackson, P.K. Prophase destruction of Emi1 by the SCF(betaTrCP/Slimb) ubiquitin ligase activates the anaphase promoting complex to allow progression beyond prometaphase, *Dev. Cell*, **2003**, *4*, 813-26.

[49] Donzelli, M.; Busino, L.; Chiesa, M.; Ganoth, D.; Hershko, A.; Draetta, G.F. Hierarchical order of phosphorylation events commits Cdc25A to betaTrCP-dependent degradation, *Cell Cycle*, **2004**, *3*, 469-71.

[50] Watanabe, N.; Arai, H.; Nishihara, Y.; Taniguchi, M.; Watanabe, N.; Hunter, T.; Osada, H. M-phase kinases induce phospho-dependent ubiquitination of somatic Wee1 by SCFbeta-TrCP, *P. Natl. Acad. Sci. USA*, **2004**, *101*, 4419-24.

[51] Li, Y.; Kumar, K.G.; Tang, W.; Spiegelman, V.S.; Fuchs, S.Y. Negative regulation of prolactin receptor stability and signaling mediated by SCF(beta-TrCP) E3 ubiquitin ligase, *Mol. Cell Biol.*, **2004**, *24*, 4038-48.

[52] Zhou, B.P.; Deng, J.; Xia, W.; Xu, J.; Li, Y.M.; Gunduz, M.; Hung, M.C. Dual regulation of Snail by GSK-3beta-mediated phosphorylation in control of epithelial-mesenchymal transition, *Nat. Cell Biol.*, **2004**, *6*, 931-40.

[53] Kumar, K.G.; Krolewski, J.J.; Fuchs, S.Y. Phosphorylation and specific ubiquitin acceptor sites are required for ubiquitination and degradation of the IFNAR1 subunit of type I interferon receptor, *J. Biol. Chem.*, **2004**, *279*, 46614-20.

[54] Hu, M.C.; Lee, D.F.; Xia, W.; Golfman, L.S.; Ou-Yang, F.; Yang, J.Y.; Zou, Y.; Bao, S.; Hanada, N.; Saso, H.; Kobayashi, R.; Hung, M.C. IkappaB kinase promotes tumorigenesis through inhibition of forkhead FOXO3a, *Cell*, **2004**, *117*, 225-37.

[55] Hayakawa, M.; Kitagawa, H.; Miyazawa, K.; Kitagawa, M.; Kikugawa, K. The FWD1/beta-TrCP-mediated degradation pathway establishes a 'turning off switch' of a Cdc42 guanine nucleotide exchange factor, FGD1, *Genes Cells*, **2005**, *10*, 241-51.

[56] Eide, E.J.; Woolf, M.F.; Kang, H.; Woolf, P.; Hurst, W.; Camacho, F.; Vielhaber, E.L.; Giovanni, A.; Virshup, D.M. Control of mammalian circadian rhythm by CKIepsilon-regulated proteasome-mediated PER2 degradation, *Mol. Cell Biol.*, **2005**, *25*, 2795-807.

[57] Kanemori, Y.; Uto, K.; Sagata, N. Beta-TrCP recognizes a previously undescribed nonphosphorylated destruction motif in Cdc25A and Cdc25B phosphatases, *P. Natl. Acad. Sci. USA*, **2005**, *102*, 6279-84.

[58] Shirogane, T.; Jin, J.; Ang, X.L.; Harper, J.W. SCFbeta-TRCP controls clock-dependent transcription *via* casein kinase 1-dependent degradation of the mammalian period-1 (Per1) protein, *J. Biol. Chem.*, **2005**, *280*, 26863-72.

[59] Bhatia, N.; Thiyagarajan, S.; Elcheva, I.; Saleem, M.; Dlugosz, A.; Mukhtar, H.; Spiegelman, V.S. Gli2 is targeted for ubiquitination and degradation by beta-TrCP ubiquitin ligase, *J. Biol. Chem.*, **2006**, *281*, 19320-6.

[60] Dorrello, N.V.; Peschiaroli, A.; Guardavaccaro, D.; Colburn, N.H.; Sherman, N.E.; Pagano, M. S6K1- and betaTRCP-mediated degradation of PDCD4 promotes protein translation and cell growth, *Science*, **2006**, *314*, 467-71.

[61] Ray, D.; Osmundson, E.C.; Kiyokawa, H. Constitutive and UV-induced fibronectin degradation is a ubiquitination-dependent process controlled by beta-TrCP, *J. Biol. Chem.*, **2006**, *281*, 23060-5.

[62] Mamely, I.; van Vugt, M.A.; Smits, V.A.; Semple, J.I.; Lemmens, B.; Perrakis, A.; Medema, R.H.; Freire, R. Polo-like kinase-1 controls proteasome-dependent degradation of Claspin during checkpoint recovery, *Curr Biol*, **2006**, *16*, 1950-5.

[63] Lobry, C.; Lopez, T.; Israel, A.; Weil, R. Negative feedback loop in T cell activation through IkappaB kinase-induced phosphorylation and degradation of Bcl10, *P. Natl. Acad. Sci. USA*, **2007**, *104*, 908-13.

[64] Ding, Q.; He, X.; Hsu, J.M.; Xia, W.; Chen, C.T.; Li, L.Y.; Lee, D.F.; Liu, J.C.; Zhong, Q.; Wang, X.; Hung, M.C. Degradation of Mcl-1 by beta-TrCP mediates glycogen synthase kinase 3-induced tumor suppression and chemosensitization, *Mol. Cell Biol.*, **2007**, *27*, 4006-17.

[65] Manavathi, B.; Rayala, S.K.; Kumar, R. Phosphorylation-dependent regulation of stability and transforming potential of ETS transcriptional factor ESE-1 by p21-activated kinase 1, *J. Biol. Chem.*, **2007**, *282*, 19820-30.

[66] van Kerkhof, P.; Putters, J.; Strous, G.J. The ubiquitin ligase SCF(betaTrCP) regulates the degradation of the growth hormone receptor, *J. Biol. Chem.*, **2007**, *282*, 20475-83.

[67] Tian, Y.; Kolb, R.; Hong, J.H.; Carroll, J.; Li, D.; You, J.; Bronson, R.; Yaffe, M.B.; Zhou, J.; Benjamin, T. TAZ promotes PC2 degradation through a SCFbeta-Trcp E3 ligase complex, *Mol. Cell Biol.*, **2007**, *27*, 6383-95.

[68] Reischl, S.; Vanselow, K.; Westermark, P.O.; Thierfelder, N.; Maier, B.; Herzel, H.; Kramer, A. Beta-TrCP1-mediated degradation of PERIOD2 is essential for circadian dynamics, *J. Biol. Rhythms*, **2007**, *22*, 375-86.

[69] Setoyama, D.; Yamashita, M.; Sagata, N. Mechanism of degradation of CPEB during Xenopus oocyte maturation, *P. Natl. Acad. Sci. USA*, **2007**, *104*, 18001-6.

[70] Seki, A.; Coppinger, J.A.; Du, H.; Jang, C.Y.; Yates, J.R., 3rd; Fang, G. Plk1- and beta-TrCP-dependent degradation of Bora controls mitotic progression, *J. Cell Biol.*, **2008**, *181*, 65-78.

[71] Soond, S.M.; Townsend, P.A.; Barry, S.P.; Knight, R.A.; Latchman, D.S.; Stephanou, A. ERK and the F-box protein betaTRCP target STAT1 for degradation, *J. Biol. Chem.*, **2008**, *283*, 16077-83.

[72] Westbrook, T.F.; Hu, G.; Ang, X.L.; Mulligan, P.; Pavlova, N.N.; Liang, A.; Leng, Y.; Maehr, R.; Shi, Y.; Harper, J.W.; Elledge, S.J. SCFbeta-TRCP controls oncogenic transformation and neural differentiation through REST degradation, *Nature*, **2008**, *452*, 370-4.

[73] Lassot, I.; Segeral, E.; Berlioz-Torrent, C.; Durand, H.; Groussin, L.; Hai, T.; Benarous, R.; Margottin-Goguet, F. ATF4 degradation relies on a phosphorylation-dependent interaction with the SCF(betaTrCP) ubiquitin ligase, *Mol. Cell Biol.*, **2001**, *21*, 2192-202.

[74] Ni, F. Recent Developments in Transferred NOE Methods, *Progr. Nucl. Mag. Reson. Spectrosc.*, **1994**, *26*, 517-606.

[75] Verdier, L.; Gharbi-Benarous, J.; Bertho, G.; Mauvais, P.; Girault, J.P. Antibiotic resistance peptides: interaction of peptides conferring macrolide and ketolide resistance with Staphylococcus aureus ribosomes: conformation of bound peptides as determined by transferred NOE experiments, *Biochemistry*, **2002**, *41*, 4218-29.

[76] Johnson, E.C.; Feher, V.A.; Peng, J.W.; Moore, J.M.; Williamson, J.R. Application of NMR SHAPES screening to an RNA target, *J. Am. Chem. Soc.*, **2003**, *125*, 15724-5.

[77] Bretonnet, A.S. Criblage d'affinité protéine-ligand par RMN et Application à la mise au point d'inhibiteurs de la créatine kinase, *PhD Thesis*, **2006**, Universite Claude Bernard - Lyon 1.

[78] Vidal, M.; Liu, W.Q.; Lenoir, C.; Salzmann, J.; Gresh, N.; Garbay, C. Design of peptoid analogue dimers and measure of their affinity for Grb2 SH3 domains, *Biochemistry*, **2004**, *43*, 7336-44.

[79] England, P.; Bregegere, F.; Bedouelle, H. Energetic and kinetic contributions of contact residues of antibody D1.3 in the interaction with lysozyme, *Biochemistry*, **1997**, *36*, 164-72.

[80] Vogtherr, M.; Peters, T. Application of NMR based binding assays to identify key hydroxy groups for intermolecular recognition, *J. Am. Chem. Soc.*, **2000**, *122*, 6093-99.

[81] Meyer, B.; Peters, T. NMR spectroscopy techniques for screening and identifying ligand binding to protein receptors, *Angew. Chem. Int. Ed. Engl.*, **2003**, *42*, 864-90.

[82] Clore, G.M.; Gronenborn, A.M. Theory and Applications of the Transferred Nuclear Overhauser Effect to the Study of the Conformations of Small Ligands Bounds to Proteins, *J. Magn. Reson.*, **1982**, *48*, 402-17.

[83] Clore, G.M.; Gronenborn, A.M. Theory of the Time Dependent Transferred Nuclear Overhauser Effect: Applications to Structural Analysis of Ligand-Protein Complexes in Solution, *J. Magn. Reson.*, **1983**, *53*, 423-42.

[84] Moller, H.; Serttas, N.; Paulsen, H.; Burchell, J.M.; Taylor-Papadimitriou, J. NMR-based determination of the binding epitope and conformational analysis of MUC-1 glycopeptides and peptides bound to the breast cancer-selective monoclonal antibody SM3, *Eur. J. Biochem.*, **2002**, *269*, 1444-55.

[85] Kooistra, O.; Herfurth, L.; Luneberg, E.; Frosch, M.; Peters, T.; Zahringer, U. Epitope mapping of the O-chain polysaccharide of Legionella pneumophila serogroup 1 lipopolysaccharide by saturation-transfer-difference NMR spectroscopy, *Eur. J. Biochem.*, **2002**, *269*, 573-82.

[86] Johnson, M.A.; Jaseja, M.; Zou, W.; Jennings, H.J.; Copie, V.; Pinto, B.M.; Pincus, S.H. NMR studies of carbohydrates and carbohydrate-mimetic peptides recognized by an anti-group B Streptococcus antibody, *J. Biol. Chem.*, **2003**, *278*, 24740-52.

[87] Kumar, A.; Wagner, G.; Ernst, R.R.; Wüthrich, K. Buildup rates of the NOE measured by 2D Proton Magnetic Resonance Spectroscopy: Implication for studies of protein conformation, *J. Am. Chem. Soc.*, **1981**, *103*, 3654-58.

[88] Nilges, M.; O'Donoghue, S. Ambiguous NOEs and automated NOE assignment, *Prog. NMR Spectrosc.*, **1998**, *32*, 107-39.

[89] Diercks, T.; Coles, M.; Kessler, H. Applications of NMR in drug discovery, *Curr. Opin. Chem. Biol*, **2001**, *5*, 285-91.

Received: April 30, 2010 Revised: September 14, 2010 Accepted: February 21, 2011

PMID: 21222584